ROYAL SOCIETY OF CHEMISTRY

PAPER

Check for updates

Controlled surface acetylation of cellulosics to tune biodegradability – expanding their use towards conventional plastics

Alistair W. T. King, [ID] *[a] Antti Paajanen, [ID] [a] Ella Mahlamäki, [ID] [a] Mikko Mäkelä, [ID] [a] Paavo Penttilä, [ID] [b] Michael Cordin,[c] Avinash Manian, [ID] [c] Mari Leino,[a] Elisa Spönla,[a] Maritta Svanberg,[a] Tetyana Koso,[a] Atsushi Tanaka,[a] Vuokko Liukkonen,[a] Amalie Solberg,[d] Anniina Savolainen,[a] Hannes Orelma,[a] Antti Korpela,[a] Kristin Syverud [ID] [d] and Ali Harlin[a]

The European Commission's single-use plastics directive has put major restrictions on the use of chemically modified cellulosics for different material applications, *e.g.*, as films, fibres, foams and other shaped objects. In addition, the wet strength and barrier properties of some of these materials are lacking, in comparison to petrochemical-based plastic materials. In the current study we demonstrate that it is possible to carry out surface selective acetylation of kraft fibre paper and nano-paper to create materials that maintain biodegradability. This is shown to be highly dependent on the degree of bulk acetylation, with those materials with modification restricted to fibril surface monoacetylation offering fine control over enzymatic digestibility. Materials which show the formation of cellulose triacetate were much less degradable in the timeframe of our assessment methods. However, the wet strength and extensibility of these materials was significantly improved, pushing the envelope for application towards moisture-rich environments. The mechanistic component of our study shows acetylation occurs down to the elementary fibril surface level, and not just on the macrofibre, or fibrillar bundle, level. We believe that this study offers a strong basis for widening the application scope of cellulosics towards traditionally petrochemical-based synthetic plastics.

Sustainability spotlight

To reduce our dependence on fossil-based value chains, cellulosics (regenerated fibres/films or native fibres) typically require further physiochemical modification, *e.g.*, increasing barrier properties, to reach specifications suitable for materials application, but also with comparable costs to melt-processed plastics. One property of cellulosics is their rapid biodegradability in the environment, which is generally viewed as beneficial. However, the ability to reduce the biodegradability of cellulosics, to increase their persistence in application, *e.g.*, in farming and fishing, will likely rapidly expand their utility. In this article we demonstrate how to control surface *vs.* bulk reactivity of paper, as a low-cost model cellulosic substrate. We show that simple 'surface acetylation' has the potential to tune biodegradability with no persistent degradation products. It is intended that these results will support the refinement of legislation and future business directions. The article is immediately relevant to the UN's sustainable development goals 11 and 13–15.

Introduction

The phenomena of the build-up of microplastics in our environment and the associated accumulation of larger plastic objects, in the earth's oceans,[1,2] has clearly illustrated the urgency for concerted changes. The European Commission has rapidly led the way in legislating changes. However, this process is of course not smooth and can be disruptive to business. Most notably the European Union Single-Use Plastics Directive 2019/904 (ref. 3) has been formulated with rather abstract definitions of what a plastic is; most notably for renewable biopolymers, the biopolymers themselves are not defined as single-use (SU) plastics. However, if they are chemically modified, then they are defined as SU plastics and, as such, must be recycled after use, or at least not disposed of in the environment. This severely limits their commercial potential and the novel material properties that modified biopolymers can potentially contribute towards materials applications, typically filled by petrochemical-based synthetic polymers, *e.g.*, as fishing and

[a]VTT Technical Research Center of Finland Ltd, Tietotie 4e, 02150 Espoo, Finland. E-mail: alistair.king@vtt.fi

[b]Department of Bioproducts and Biosystems, School of Chemical Engineering, Aalto University, Vuorimiehentie 1, 02150 Espoo, Finland

[c]Research Institute of Textile Chemistry and Textile Physics, University of Innsbruck, Hoechsterstrasse 73, 6850 Dornbirn, Austria

[d]RISE PFI, Høgskoleringen 6b, 7491, Trondheim, Norway

farming materials (fibres, netting and mulches). Quoting from the directive (Article 3, point 1): *''plastic' means a material consisting of a polymer as defined in point 5 of Article 3 of Regulation (EC) No 1907/2006, to which additives or other substances may have been added, and which can function as a main structural component of final products, with the exception of natural polymers that have not been chemically modified;'*. Note that there is no room for distinction between types of chemical reagents (ethers, esters, *etc.*), regioselectivities (2, 3, or 6-hydroxyl functionalisation, in the case of celluloses repeating glucose residue) or spatioselectivities (fibril or fibre surfaces *vs.* bulk functionalisation). The SU plastic definition has reportedly come about through heavy lobbying from industry and has led to frustration and deep critisism from the scientific community, due to the abstract nature of the definition. Therefore, there is some confusion and rhetorical potential surrounding this legislation. For example, the definition does not rely on the traditional technical adjective definition of 'plastic', as it does not mention melting points or glass transitions. Moreover, rigid biopolymers such as cellulose, typically require very heavy bulk chemical modification to become 'plastic'. The practical relevance of these criticisms regarding biodegradation (from the EC perspective) is not clear but obviously the legislation has to rely on simple and practical definitions to avoid future complications and confusion.

Fortunately, the directive will be reviewed in 2027 (see Article 15). This will give manufacturers and scientists time to develop suitable protocols for a more accurate specification of biodegradability and a better mechanistic understanding of biodegradation for conceptual materials, that can be designed to have minimal ecosystem impact. Through a more detailed review of the current legislation (SI Section 1), directives and strategies of the European Commission, designed to limit the negative impacts of plastics, covalent (surface or bulk) modification of biopolymers is currently not considered at all (as multi-use plastic materials), or even as viable options for plastic replacement or barrier materials, through spatioselective (surface) chemistry. One clear bulk application which uses paper and board, but which still requires enhanced barrier and surface properties, utilises dispersion or extrusion coating, where typically synthetic polymer/oligomer fragments are bound to the surface of paper and board, but not directly covalently attached. For cases such as these, Regulation (EU) 2024/2770 (ref. 4) sets limits on the biodegradation rate of polymer additives, for this and other applications. Whereas Decision (EU) 2019/665 (ref. 5) limits these additives to a maximum of 5% by weight, of the total packaging weight.

One key example, that may have led to ambiguity in defining legislation, which will have a significant impact on industry, is the use of cellulose acetate (CA) in cigarette filters. Cigarette butts are commonly disposed of in water ways and on pavements. The filters are typically made of high degree of substitution (DS) CA fibre. An early report erroneously identified CA as non-biodegradable,[6] without extensive work on the topic. A more recent review[7] has reiterated the clear decrease in biodegradability of CAs, as DS increases, based on a combination of the key literature studies. Drawn from an existing body of

research, dedicated to understanding all aspects of CA's biodegradation,[8] it is also important to highlight that previous work even indicates that high DS CA, close to cellulose triacetate (CTA), is actually biodegradable over longer time periods – recent studies show this is possible even under seawater conditions, indicating that the long-term impact from CA towards microplastics may be limited.[9] Therefore, more needs to be done, as soon as possible, to guide the best courses of action for updating related legislation.

While bulk acetylation to high DS clearly has an impact on rapid biodegradability, we started our own research into this topic with the hypothesis that *'restricting chemical modification to only cellulose surfaces will have a limited impact on biodegradation, in comparison to a bulk-modified sample'*. In this manuscript we attempt to prove this hypothesis, using paper as a key commercial substrate and acetylation as a model reaction. Papers (traditional macro- and nano-papers) were chosen, as low-cost established materials that may offer a substitute to traditional petrochemical plastic-based packaging or barriers, without relying on multi layering.

Indeed, acetylation of paper has been used in the past, also commercially. Acetylated paper has found use in preparatory chromatography, where the more hydrophobic acetylated paper acts as a stationary phase for selective retention of molecules against organic solvent mobile phases.[10] Electrical insulation papers have also taken advantage of acetylation, to increase the thermal stability of separators in electrical contact.[11] Many reports exist into the use of acetylated papers, nanopapers and cellulosics in general. However, few deal with the issue of biodegradation or more specifically, the tunability of biodegradation.

Materials and methods

Acetylation reaction conditions

Bleached softwood kraft paper hand-sheets and CNF nanopaper hand-sheets were cut to either 5×5 or 10×10 cm^2. The sheets were soaked in different vol% compositions of acetic anhydride to pyridine $(25:75, 62.5:37.5 \& 100:0)$. They were then removed from the solutions and placed individually into appropriately sized plastic Petri dishes. A small reservoir of the acetylation mixtures was placed in the corner of the Petri dish to maintain a positive atmosphere of acetylating mixture, to avoid drying and caramelisation of the sheets. The Petri dishes were
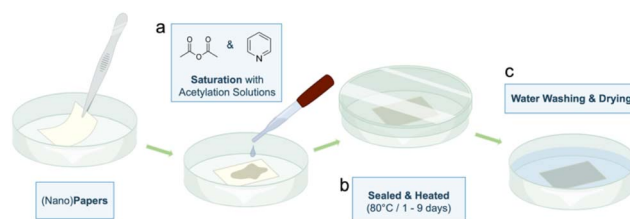

Fig. 1 Laboratory procedure for acetylation of the (nano)paper hand-sheets. The individual steps involve (a) saturation with the acylation solution. (b) 'Ripening' (heating) for the appropriate time. (c) Final washing and drying.

topped with lids and thoroughly sealed with Teflon tape. These were placed in a laboratory oven at 80 °C for 1 to 9 days. The reactions were quenched by soaking the sheets in a water bath for 18 h (×2), followed by drying the wet sheets in a fume hood, in open containers (Fig. 1).

Results and discussion

Surface *vs.* bulk reaction optimizations

A (statistical) design of experiments (DoE) approach was used to study the liquid-state acetylation of bleached softwood kraft (BSK) hand-sheets. The central composite design (Fig. 3a) included two variables, reaction time (1, 5 & 9 days at 80 °C) and vol% composition of acetic anhydride (Ac_2O, with the rest pyridine), and required a total of 11 experiments. Reactions were performed by soaking the sheets in the acetylation media and 'ripening' the mixture in a laboratory oven, followed by washing (Fig. 1).

Three representative samples of varying DS and regioselectivity of reaction were made on a larger scale for extended characterisation. The generated samples were analysed using a range of methods (SI Table S2), and the degree of substitution (DS) and % weight loss from enzymatic digestibility ($\%_{ENZ}$) were modelled with multiple linear regression to describe the evolution of sample properties as a function of the acetylation conditions, using response surfaces. Suitable reaction conditions were initially optimised using attenuated total reflection infrared (ATR-IR) spectroscopy, as a rapid method for visual assessment of reaction efficiency. ATR-IR is also currently not the ideal method for mechanistic studies, due to limitations in sample penetration depth. The bulk DS and regioselectivity of reaction was followed using a novel solution-state NMR protocol.[12] This is clearly illustrated by comparing the acetate regions (~2 ppm) in the diffusion-edited ^1H spectra for the representative samples, with varying reaction conditions (Fig. 2) – by peak fitting (using *fityk*[13]) the 6-OAc (mono and diacetate) *vs.* the 6-OAc (CTA), a value for % selectivity for CTA ($\%_{CTA}$) can be calculated (SI Section 3.3). Mild reaction conditions (100 vol% Ac_2O – 1 day) showed formation of 6-acetate under non-catalytic conditions (no pyridine), consistent with fibril surface only reactivity, as has been demonstrated previously.[14,15] The pyridine-containing mixtures (62.5 vol% – 1 day & 25 vol% –

5 days) show the formation of CTA, consistent with the topochemical transformations involved in commercial bulk catalytic heterogeneous acetylations.[16,17] Multiplicity-edited heteronuclear single-quantum correlation (HSQC) nuclear magnetic resonance (NMR) spectroscopy for the intermediate conditions, using the 62.5 vol% − 1 day hand-sheet (Fig. 2b), clearly showed the presence of 2 & 3-acetylation, consistent with previous literature assignments[18] and supporting the apparent diffusion-edited ^1H NMR selectivity, shown (Fig. 2a). After preparation and NMR analysis of the full DoE array of samples (Fig. 3), it is clear that it is possible to prepare samples where 6-acetylation is restricted to cellulose surfaces, as was also observed and calculated for milder gas-phase reaction conditions for the acetylation of a wider range of cellulosic substrates.[19] Alternatively, depending on reaction conditions, it is also possible to induce a bulk topochemical conversion of crystalline cellulose – yielding CTA domains while still retaining unmodified crystalline cellulose of close-to-native crystallite size. This was further supported by wide-angle X-ray scattering (WAXS) analysis of the representative samples (Fig. 3c). The diffractograms for the representative samples illustrate a progression to lower degrees of crystallinity, for harsher reaction conditions, by the reduction of signal intensity of the typical cellulose I_β diffraction peaks.[20] The main cellulose I diffraction peak, the 200 peak (22.5°), corresponds to diffraction from the crystallographic planes formed by the hydrogen-bonded sheets of cellulose chains. The peak width gives an indication of the fibril size, perpendicular to those planes, based on the use of the Scherrer equation.[21] After peak-fitting using *fityk* (SI Section 4.3), the 200 crystal size (L_{200}) is observed to decrease (from 5.3 to 4.5 nm), as the CTA composition increases. However, the decrease is not as significant as one might expect, based on a maximum bulk DS value of 0.74, for the more highly acetylated sample, indicating that there are some elementary fibrillar aggregates which prevents access to or swelling of all fibrils. Calculation of crystallinity index values from the WAXS data, using one of the choice methods,[22] was not performed due to the potential for error from the appearance of CTA diffraction peaks.

After these results, it was clear that a representative set of samples was available for biodegradation studies, to test the effect of a controlled surface modification. In addition, acetylation of cellulose nanofibril (CNF)-based nano-paper samples
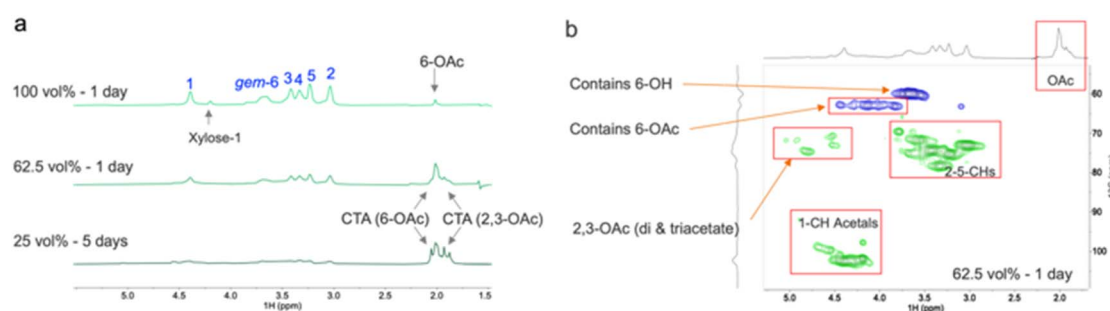

Fig. 2 Regioselectivity of the representative samples through solution–state NMR analysis. (a) Diffusion–edited ^1H NMR analysis showing the 2,3,6-OAc regioselectivity pattern in the acetate region (2 ppm), (b) multiplicity-edited HSQC spectrum for one of the key samples, as an additional method of confirming the regioselectivity.
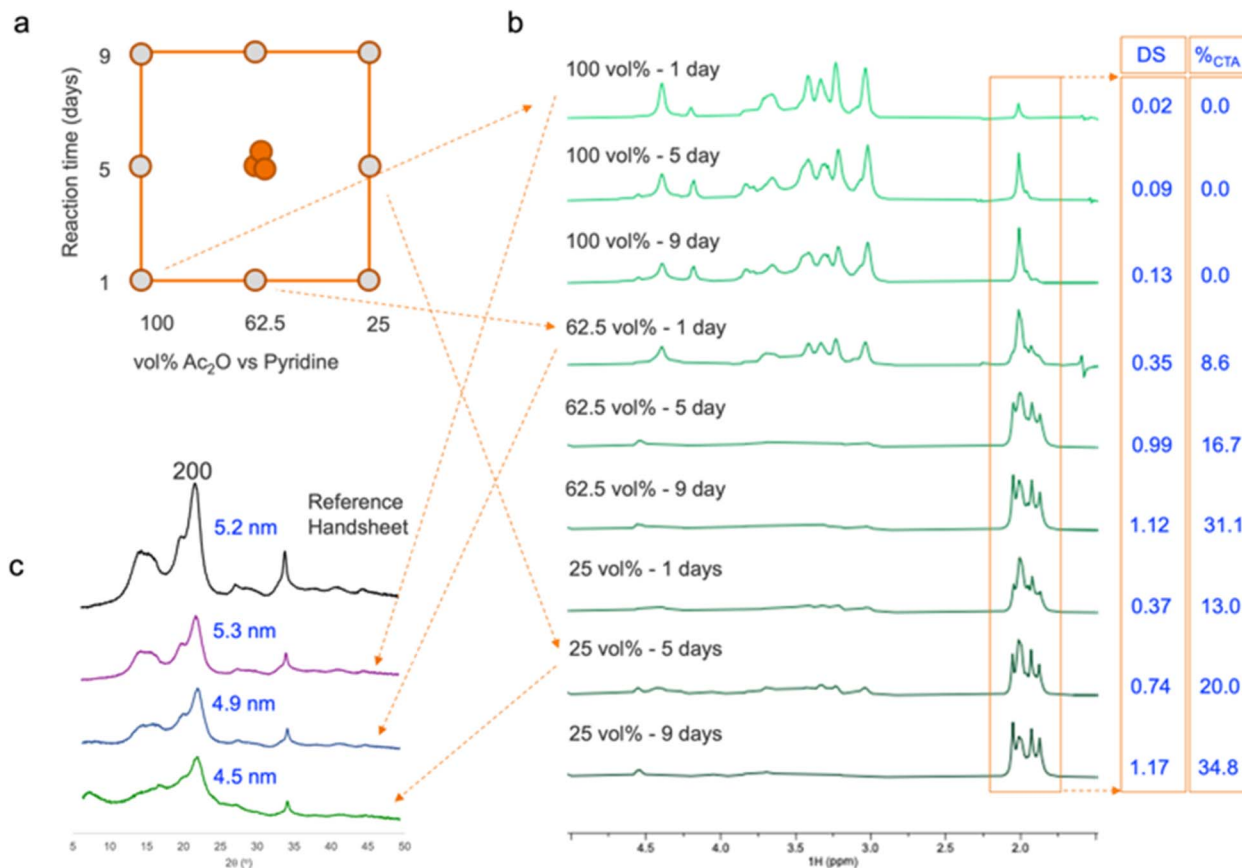
Fig. 3 NMR & WAXS analysis of key acetylated hand–sheet samples. The reaction regioselectivity is controlled by variation of the pyridine content in the acetylation mixture and reaction time. (a) Whole sample DoE matrix, (b) diffusion–edited ^{1}H spectra for the whole DoE matrix, allowing for extraction of the bulk DS and the $\%_{CTA}$ selectivity (in blue), (c) WAXS for the three representative samples against the unacetylated reference, with the L_{200} (cellulose I crystallite sizes) calculated (in blue).

was also performed, and representative samples of the macro- and nano-paper samples were made on a large enough scale for soil biodegradation studies. Quantitation of the DS for all paper samples was performed using quantitative ^{1}H NMR and diffusion-edited ^{1}H NMR (SI Section 2.4).

Spatioselectivity & mechanisms of reaction

Small-angle X-ray scattering (SAXS) experiments were carried out to detect the effects of the acetylation treatment on the morphology of nanoscale cellulose fibril structures (Fig. 4). The results showed clear and systematic differences due to the acetylation treatment and its harshness. In the dry state, the elementary fibrils stayed further apart from each other in the acetylated samples compared to the reference paper. When the samples were saturated with water, the elementary fibril bundles in the reference sample swelled more than those in the acetylated samples. These systematic differences, due to the acetylation treatment observed both in wet and dry states, show that the acetylation treatment has a clear effect on the structure of the paper at the level of the elementary fibrils (diameter of some nanometres), indicating that the reaction took place at least partially at the elementary fibrillar surfaces, within the

fibrillar bundles. Naturally the acetylation also occurs on the outer fibrillar bundle surfaces.

To compare with the scattering and NMR studies and illustrate the mechanism of acetylation, a fibrillar bundle geometry was prepared (Fig. 5) to contain different degrees of surface acetylation throughout the fibrillar bundle. Different mechanisms were assumed where: (A) low DS regioselective 6-OH acetylation occurs at most fibril surfaces, except for some surfaces within fibrillar aggregates, and (B) topochemical full fibril conversion to CTA occurs, as observed in the presence of pyridine, which is consistent with the acid-catalysed mechanism, mechanistically elaborated by Sassi & Chanzy.[17] This latter mechanism at high DS (increasing pyridine contents), where full fibrils are converted to CTA, is also evident from the formation of a diffraction peak in the wide-angle region at a 2θ value of 9° (Fig. 6b), especially for the 25 vol% sample – this resembles the (010) plane from the CTA I literature structure[23] (Fig. 6a, b, 4a and b) and is not associated with the known native hydrated crystalline cellulose II allomorph, which also has a diffraction plane separation at a similar d-spacing.[24]

Moreover, the CTA diffraction peak appears in both the dry and wet states, as evident by the scattering peak at $q = 5.5$ Å^{-1} in
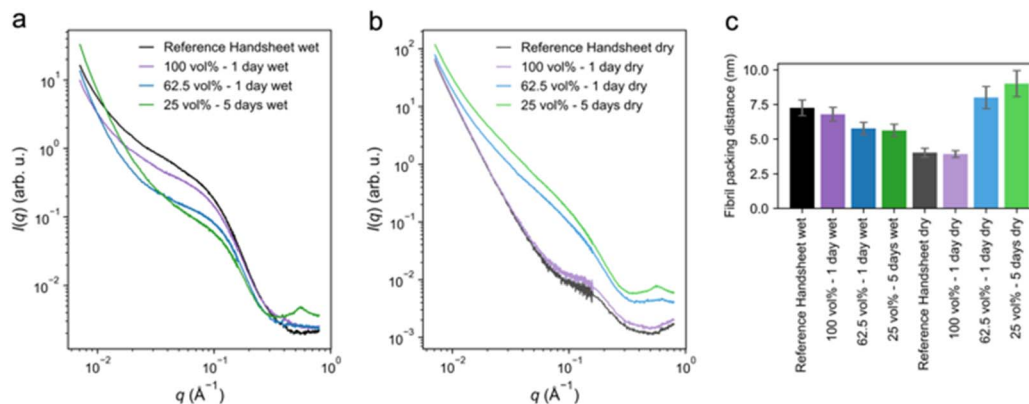
Fig. 4 SAXS results for the dry and hydrated (acetylated and reference) paper hand sheets. (a) SAXS intensities for the hydrated samples. (b) SAXS intensities for the dry samples. (c) Distance between elementary fibrils, as determined from the location of the peak maximum in the Kratky plots (SI Fig. S8).
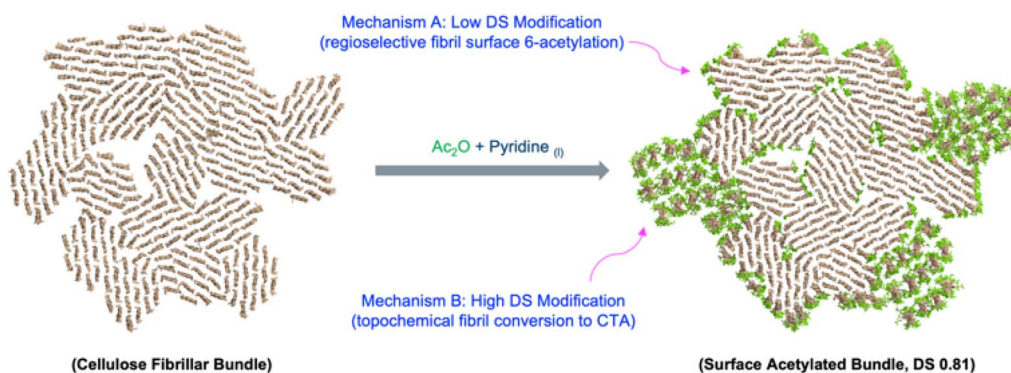

Fig. 5 Proposed spatio- & regioselective directing mechanisms for acetylation through fibrillar bundles – cross-sectional models are prepared through geometry modelling tools and dynamics simulations (SI Section 2) – the acetate groups are shown in green.
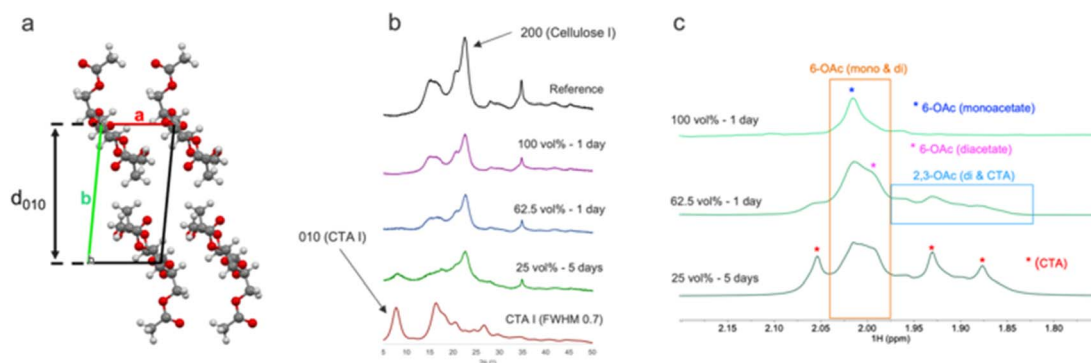

Fig. 6 Appearance of the CTA I (010) X-ray diffraction plane, in WAXS concomitant with CTA formation from comparison with NMR. (a) CTA I crystal structure with the (010) d-spacing highlighted. (b) Comparison of the experimental WAXS samples with a calculated diffraction pattern for CTA I (FWHM of 0.7). (c) Assigned acetate region in the diffusion-edited ^{1}H NMR spectra.

Fig. 4a and b. The longer interplanar distance corresponds to the extended separation of the repeating sugar units by the increased steric repulsion, between equatorial acetate groups – as opposed to the shorter distance unit separation by interchain equatorial H-bonds, in the native cellulose I allomorph. This diffraction peak is at slightly shorter d-spacing than the literature structure, and the Scherrer length (crystallite size) is clearly rather short (<4 nm) but still abundant enough at these lengths to give a defined diffraction peak. Appearance of this peak is also concomitant with an increase in %$_{CTA}$ selectivity for the 3 representative samples (Fig. 6c) from low to high (0.0, 8.6 & 20.0). Considering that topochemical conversion to crystalline

CTA has been observed for the Sassi & Chanzy acid-catalysed system[17] and that we do not observe drastic changes in the relative intensities of the cellulose I peaks at high DS (Fig. 3c), it seems logical that a similar topochemical conversion, *i.e.*, retention of some cellulose I allomorph structural motifs, of whole elementary fibrils is occurring in our case.

In terms of spatioselectivity over the nano- to micro-scale, few methods exist that give good resolution. Clearly optical and tomography-based methods have limited spatial resolution. However, NanoIR-AFM is a powerful technique to measure IR spectra with superior spatial resolution, compared to other techniques.[25–27] Although an exact specification of the resolution is difficult due to its special underlying physics, it is generally assumed that a sub-100 nm resolution is possible. Therefore, this technique is suitable to analyse the variation of DS along the cross-section of the (partially) acetylated paper, namely from the surface to the inner part of the paper. In the initial stage, utilizing a conventional IR spectrometer, IR spectra of samples with diverse DS were measured and analysed to comprehend the correlation between DS and the height of diverse IR peaks (SI Fig. S10). The relation between the degree of acetylation of cellulose and the corresponding ATR-IR spectra were already described in the scientific literature.[28] For comparison, nanoIR-AFM spectra of pure cellulose and pure cellulose triacetate are shown in SI Fig. 11. Note, that due to the different physics of this measurement technique, the height relation between different peaks can be significantly different, compared to spectra of conventional IR spectrometers. The analysis of the IR spectra in SI Fig. S1 & S11 indicates that, in particular, the IR peaks at wavenumbers of 1740–1750 cm^{-1} and 1640 cm^{-1} are suitable to gain information about the relative DS of the corresponding sample.

Fig. 7b shows an AFM height image along a line of the cross-section of a selected sample (25 vol% – 5 days). At each blue point, shown in the AFM height image, a nanoIR-AFM spectrum was measured. The AFM measurement indicates that the roughness (and porosity) of the paper is high; in principle, these are no good precondition to measure nanoIR-AFM spectra of good quality. The resulting strong variation of the interaction between the paper's material and the AFM cantilever tip induces a corresponding variation of the measured signal intensity. It appears that this variation overlaps strongly those variations in the IR signal intensity that are caused by the chemical contrast in the sample.

The strength of the cantilever vibration depends not only on the amount of IR light absorbed by the sample, but also on how well the sample can transfer this excitation to the cantilever. Consequently, the 'intensity' of all excited vibrations over the whole wave-number range of a measured IR-spectrum was integrated and was regarded as a representative of the strength of the interaction between the paper and the AFM cantilever system. These calculated values were used to normalize the corresponding IR spectra. Fig. 7a shows a plot of all measured nanoIR-AFM spectra over the cross-section (see Fig. 7b) of the selected paper. As already mentioned, in principle, the peak at the wavenumber 1740–1750 cm^{-1} is more intense, the larger DS is, and the peak at 1640 cm^{-1} is more intense, the smaller DS is. The analysis of these two peaks over the length of the paper's cross-section indicates that there are variations in the DS, but there does not appear to be a monotonic decrease in degree of acetylation with increase in depth through the paper.

With the current nanoIR-AFM data, it is clear that the acetylation across the paper surface is relatively uniform. In the future efforts will be made to assess the spatioselectivity of acetylation across the individual pulp fibre surfaces. This will require a good deal more experimental protocol development but will be invaluable in understanding the reactivity of different fibrous cellulosic materials.
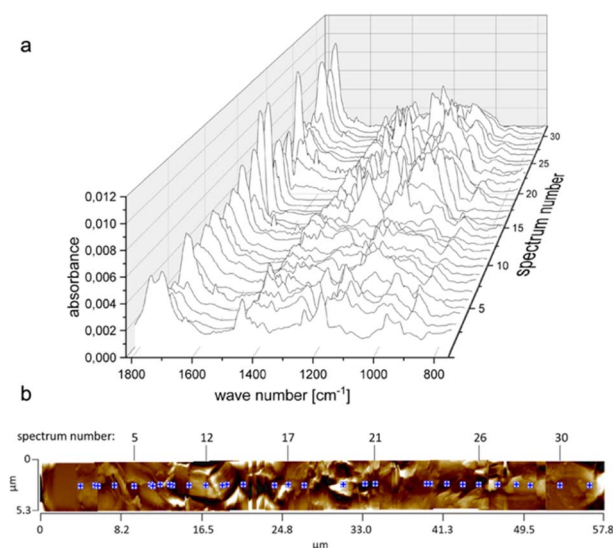

Fig. 7 NanoIR-AFM analysis of the 25 vol% – 5 days acetylated paper cross-section. (a) Plot of all measured nanoIR-AFM spectra along the cross-section of the selected sample, specified by the blue points in the AFM height image of (b). The peak height at a wavenumber of 1740–1750 cm^{-1} represents the DS, whereby, at a wavenumber around 1640 cm^{-1} no clear peak is recognizable. (b) AFM height image of the cross-section across the entire thickness of the specimen. An area of 5.3 μm × 57.8 μm was measured, where the bottom scale denotes distances from one face of the paper sample (at 0 μm) to the other face, through the thickness. The colour variations in the image are representative of variations in height, from low (dark) to high (light). The error in the IR signals is discussed in SI Section 5.
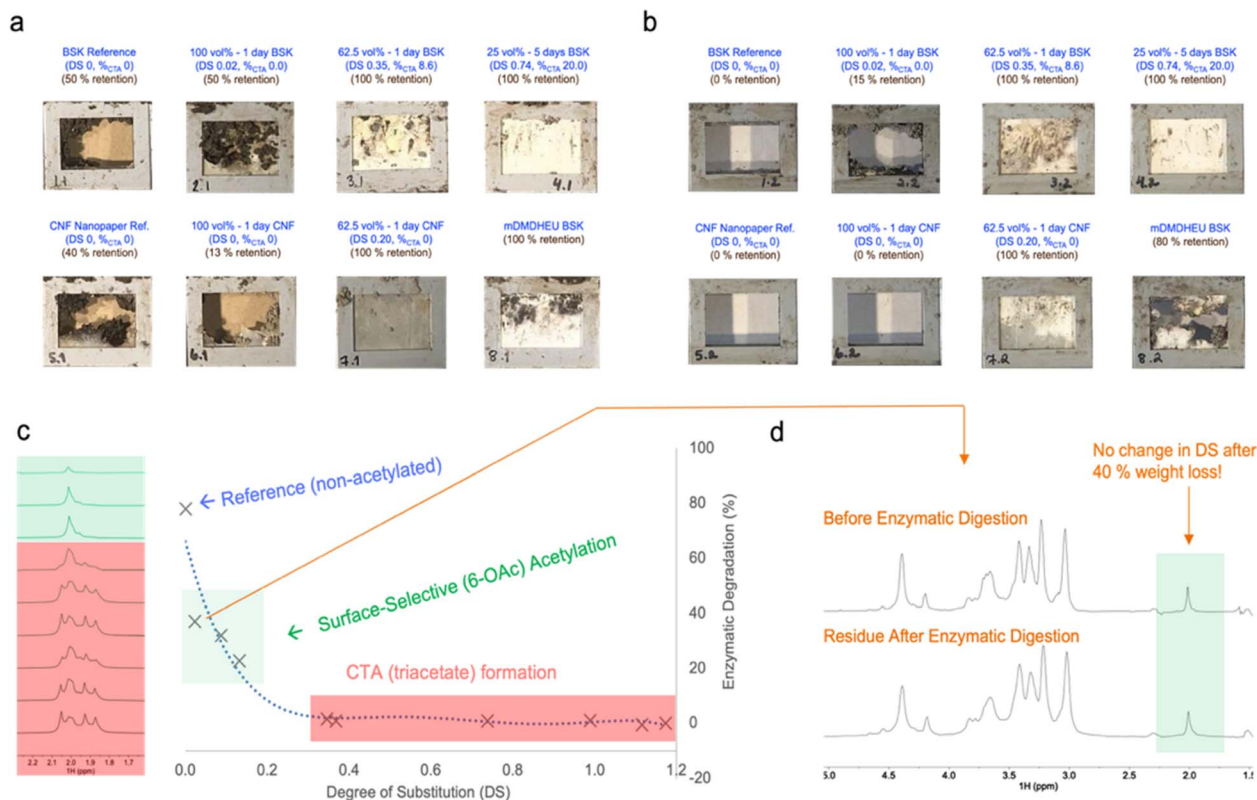
Biodegradation studies

Larger representative samples were degraded using a soil biodegradation assay, with sampling at 1 and 3 months (UEN EN 13432:2001, Fig. 8a and b). Both the macro- and nano-paper samples were tested. For comparison, a 1,3-dimethylol-4,5-dihydroxyethylene urea (mDMDHEU) cross-linked BSK handsheet[29] was also tested, to see the effect of introduction of a cross-linking reagent, without affecting the overall surface 'hydrophobicity' of the sample – as is expected with acetylation. Images of the residual samples after the soil tests, and the rough values for paper retention (average of a duplicate experiment) after 1 or 3 months, are given in Fig. 8a and b. A rapid enzymatic method[30] was also used to develop an accessible digestibility parameter/scale (Fig. 8c and d), for the regression

Fig. 8 Soil and enzymatic biodegradability of the acetylated and cross-linked samples. (a & b) Soil biodegradability's over 1 & 3 months – % retention values are the % area of the surfaces that are retained after the allotted time-period. (c) Enzymatic biodegradability vs. the increasing DS and regioselectivity of acetylation. (d) Diffusion-edited ^{1}H NMR analysis of the 62.5 vol% – 1 day sample, before and after enzymatic digestion – showing no significant change in degree of bulk acetylation after solids recovery.

model, as the current soil studies do not provide accurate numerical data, as the kinetics are too slow to allow for complete digestion of high DS acetate samples, within a suitable experimental timeframe. This protocol[30] was used, as it was already correlated against pilot-scale composting of different cellulose and cellulose ester-based films.

From these results, it is clear that the soil biodegradability of the macro-papers suffers drastically with the formation of CTA (Fig. 8a and b), at least over these short time periods. Even the 62.5 vol% nano-paper sample, with a DS of 0.20 and no CTA formation, shows poor soil biodegradability at 3 months. Thus, CTA formation is only one factor in significantly reducing soil biodegradability, potentially with low porosity (as demonstrated with nano-papers) being a significant secondary factor. The lower DS 6-acetylated macro-paper sample does indicate some potential resistance to degradation, compared to the reference sample, but is almost completely consumed by the 3-month mark. Surprisingly, the mDMDHEU cross-linked BSK paper sample also shows strong resistance after 1 month in soil but shows clear signs of degradation, in comparison to the CTA-containing samples, after 3 months. Due to the higher expected 'hydrophobicity' of the CTA-containing samples, it is clear that both hydrophobicity and cross-linking can prevent significant swelling of the sample, which may affect the initial penetration of the matrices with degrading microorganisms or enzymes.

From Fig. 8c, it is very clear that the enzymatic digestibility of the acetylated papers is significantly impeded by the presence of CTA, with the 6-acetylated only (no CTA) samples still allowing for considerable weight-loss during the experimental time frame. It is important to note that the enzyme cocktail that is used does not contain esterases to catalyse deacetylation (potentially increasing local swelling), which has been proposed as a key initial step in biodegradation of high DS acetate.[8] Thus, the weight loss is solely based on the action of polysaccharide-fragmenting enzymes. As such, it was surprising to note that the DS of acetylation of the residual paper did not change after 40% enzymatic weight loss. This indicates that at the lower DS values, in the absence of CTA, the enzymes either digest both the partially acetylated and unmodified polysaccharides, or the low DS surface chains become soluble in the media after enzymatic digestion of surrounding unmodified polysaccharide. This is not totally unexpected as low DS cellulose acetate (DS ∼0.5–1) is known to be water soluble,[31,32] and indicates that the low DS materials are rapidly degradable in aqueous environments.

Overall, in the absence of more detailed soil and seawater mechanistic studies, the CTA composition clearly has a significant effect on penetration of digesting agents into the bulk fibrillar bundles, acting as a physical barrier. Further dissection of this mechanism needs to be done, in particular, concerning

the formation and degradation of possible residual agglomerated microparticle-like species at the later stages of soil, compost and seawater digestion studies. Further to this, future enzymatic digestibility studies should attempt to include esterases and possibly oxidising enzymes to facilitate fracture of hydrophobic ester surfaces on fibres and fibrils.

Film properties

The overall physiochemical data is presented in Table 1, including previous chemical analyses. Of course, the dependence of the penetration of the film surfaces with aqueous-born species will be visible from the contact angle (CtA) measurements (Fig. 9). It seems that even with a very low DS of 0.02, with only 6-acetylation, there is some modest increase in the CtA, with the samples wetting immediately. This obviously will have a predictable effect on the penetration of the papers with water-mobile degrading species and there will be an expected reduction in the initial kinetics of degradation, based on this phenomenon. For the higher DS samples, with formation of CTA, the CtA values increase significantly and take much longer (up to 1 hour) to wet completely. From analysis of the stress–strain properties, the wet strength clearly suffers for the low DS samples. This will have a major effect on the mechanical dispersibility of the materials under different conditions. One interesting feature is that the formation of CTA has a significant effect on the wet strength and extensibility of the materials. This phenomenon has been observed previously,[33] where they propose that the formation of covalent cross-linkages is the likely mechanism of increased wet strength. This is somewhat speculative as acid-catalysed acetylation conditions are unlikely to cause the formation of cross-links. Based on our results, we propose that there is a semi-continuous elastic CTA phase formed, in the fibrillar bundles (Fig. 5), resulting from the high DS acetylation conditions. This yields more extensible and strong materials and is formed through a topochemical conversion mechanism, occurring along the cellulose I elementary fibril lengths. While the water barrier and
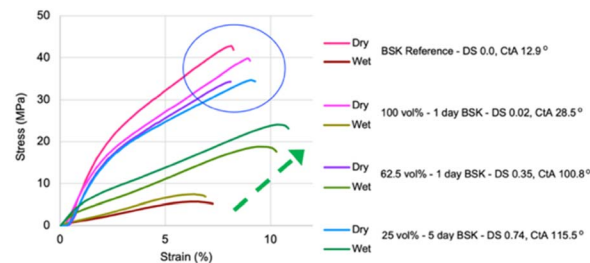

Fig. 9 Stress–strain properties for the different representative acetylated BSK hand-sheets. The DS and CtA values are shown for each sample.

mechanical properties for the low DS 6-acetylation sample do not show a very significant improvement, higher homologue esters may have a significantly enhanced effect at the same DS values and surface selectivity. This is already indicated in a recent article concerning tensile and wetting properties of regenerated cellulose ester films, from homogeneous modification.[34] Their results indicate that with much lower DS values for the much higher ester homologues, CtA values are even higher than the commercial CA films (DS 2.5) – while elongation of the dry films of the higher homologues can be enhanced significantly (albeit with reduction in stress at break). Another dimension, beyond the barrier and strength properties is the addition of highly novel functionalities that require only a small active component. In these cases, biodegradation most likely is also highly tuneable, yet may still fall under the multiple use category, under the current (2014) legislation definitions.

Response surfaces

Linear regression models were determined to link the reaction conditions (% acetic anhydride *vs.* pyridine & reaction time) to the tunability of the biodegradability based on determined DS and enzymatic digestibility. The quadratic regression equations were refined by excluding insignificant model coefficients using

Table 1 Full physiochemical data from the analysis of the reference and modified samples

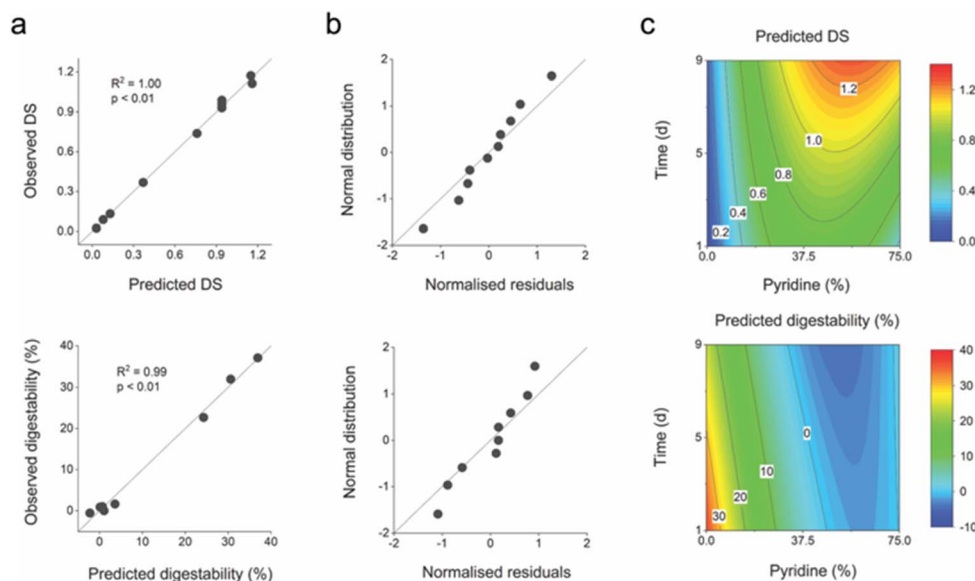| Sample	DS	$\%_{CTA}$ (%)	$L_{(200)}$ (nm)	Enzymatic degradation (%)	Stress (dry/wet, MPa)	Strain (dry/wet, %)	Tensile index (dry/wet, Nm g^{-1})	Contact angle (°)
BSKP paper (unmodified)	0	—	5.2	78.0	42.7/5.2	8.2/7.3	50.2/6.1	12.9
CNF nanopaper (unmodified)	0	—	—	—	—	—	—	—
100 vol% – 1 day (BSK)	0.02	0.0	5.3	37.1	39.8/7.0	8.9/6.9	46.8/8.2	28.5
100 vol% – 5 days (BSK)	0.09	0.0	—	32.0	—	—	—	—
100 vol% – 9 days (BSK)	0.13	0.0	—	22.7	—	—	—	—
62.5 vol% – 1 day (BSK)	0.35	8.6	4.9	1.6	33.2/18.1	8.3/10.2	39.1/21.3	100.8
62.5 vol% – 5 days (BSK)	0.99	16.7	—	1.0	—	—	—	—
62.5 vol% – 9 days (BSK)	1.12	31.1	—	−0.6	—	—	—	—
25 vol% – 1 day (BSK)	0.37	13.0	—	0.9	—	—	—	—
25 vol% – 5 days (BSK)	0.74	20.0	4.5	0.9	34.4/23.7	9.3/10.7	40.5/27.9	115.5
25 vol% – 9 days (BSK)	1.17	34.8	—	0.0	—	—	—	—
100 vol% – 1 day (CNF)	0.01	—	—	—	—	—	—	—
62.5 vol% – 1 day (CNF)	0.45	—	—	—	—	—	—	—
mDMDHEU (BSK)	0	—	—	—	—	—	—	—

Fig. 10 Response surfaces for acetylation DS and enzymatic digestibility. (a) Observed *vs.* predicted properties. (b) Normalised model residuals. (c) Predicted response surfaces, linking reaction time and Ac$_2$O:Pyr vol% ratios, to the degree of substitution (above) and enzymatic digestibility (below).

a *t*-test, which compared the coefficients against the model residuals on a significance level $\alpha = 0.05$. The final models included the same model coefficients, *i.e.*, the main effects, their interaction, and the quadratic term for acetic anhydride *vs.* pyridine ratio and explained 99–100% of the variation in the measurements (Fig. 10a). Only one DS observation was identified as an outlier based on normalised model residuals and was thus excluded from the final model. This exclusion increased the predicted R^2 value from 0.81 to 0.98 based model on cross-validation but did not considerably change the interpretation of the response surface (Fig. 10c). The ANOVA tables of the two regression models and their regression equations are given in the SI (Tables S4, S5, eqn (S2) & (S3)).

The predicted response surfaces shown in Fig. 10c indicated an antagonistic relationship between DS and enzymatic digestibility within the experimental design range and can be used to interpret the tunability of biodegradation based on acetylation conditions. Predicted DS increased toward high pyridine ratios and long reaction times, which considerably decreased the enzyme-catalysed hydrolytic weight loss compared to the non-treated reference sample and bulk DS samples in the range below 0.2. Thus, there clearly is a narrow window where there is fine control over the rate of enzyme-catalysed hydrolytic weight loss, with longer digestion times out of the range and, most likely, predictive accuracy of this protocol.

For the purposes of this study pyridine was used, only as it is a classical reagent used in a catalytic to stoichiometric fashion. Clearly, it is not without its hazards though. Fortunately, there are also a wide range of organic and inorganic bases available that have more favourable hazard profiles. However, it seems that reaction even using only liquid Ac$_2$O, in the absence of pyridine, allows for fine control over the enzymatic digestibility.

And, to achieve significant changes in %$_{\text{ENZ}}$, pyridine is not actually required.

Conclusions

At the beginning of this study, we aimed to prove that a spatio-selective surface modification by esterification would allow for alteration of material properties but still allow for biodegradability. As such, this could be used to inform current legislation and future analytical development to avoid environmental hazards. It seems that by fine control over reaction conditions, it is possible to restrict acetylation to fibril surface chains and that this already has a significant impact on the enzymatic digestibility, despite that the acetylated surface layer is thin and is a minor structural/volume component of the bulk paper fibres. Even acetylation on fibril surfaces to a bulk DS of 0.02, where only 6-OHs are acetylated, results in a minor increase in the CtA. No major changes in mechanical properties (dry or wet) are apparent. Since there is only a minor increase in the CtA, compared to the reference paper, at these very low bulk DS values, the reason for the major changes in enzymatic digestibility are not yet clear. However, variation in swelling, due to reduced interfibrillar H-bonding, would allow for changes in the accessibility of the interior fibrils to enzymes.

At higher bulk DS values, where CTA domains form, this restriction in swelling is most pronounced. There are also major increases in the CtA values, preventing penetration into the fibre network. In these cases, the formation of defined CTA domains, is likely acting as a 'glue' holding the fibre network together, preventing swelling. In both the high and low DS cases, unmodified crystalline fibrillar aggregates are retained – low DS acetylation is restricted to fibril surfaces, and the high DS acetylation shows clear separation of CTA and crystalline

cellulose fibrillar aggregate domains. Therefore, full bulk topochemical conversion is not apparent here but likely possible at higher temperatures. Thus, the regioselectivity and spatioselectivity of the reactions can be controlled – with clear variation in material properties.

A clear drop in both soil and enzymatic digestibility is observed for those samples with CTA formation. Fortunately, old[8] and new[9] studies do show that high DS cellulose acetates can be fully biodegradable, over an appropriate timeframe. Therefore, the action of redox or esterase species in nature likely has a significant part to play in creating sites, increasing accessibility of the fibre surface or bulk fibre network towards further enzymatic or hydrolytic attack. This is supported by a recent publication[35] where impregnation of lipase has a catalytic effect on cellulose acetate degradation, under composting conditions. An additional inclusion of redox enzymes would then be a logical addition, if possible, broadening the substrate scope.

Clearly control over the biodegradability is possible, which offers the unique potential for the use of shaped cellulosic objects to replace traditional petrochemical melt-processed plastic objects. In this manner, the degradability of cellulosic materials in the environment is clearly tuneable, as is the possibility to tailor biopolymers to fully degrade after the expected lifetime in application.

While the model reagents and methods used in this study are not designed to be easily scalable for wide application, at low-cost, suitable alternatives will become available. For example, gas-phase chemistry can minimise costs. The application of longer chain ester homologues may reduce the need for extensive surface modification, increasing atom efficiency.

To design suitable multi-use materials, with enhanced properties based on natures choice, many avenues are available. Further detailed mechanistic studies are needed to support the development of lasting legislation, involving fine control over chemistry combined with biodegradation studies.

Author contributions

A. W. T. K. conceived of the overall concept, wrote the manuscript and carried out much of the data analysis; A. P. carried out the molecular dynamics work and consulted on the interpretation of data, and editing the manuscript; E. M. and M. M. consulted on and carried out the design of experiments work; P. P. processed/consulted on the interpretation of the SAXS and WAXS data and helped on the overall interpretation and writing of the manuscript. M. C. and A. M. collected and processed the NanoIR-AFM results; M. L. carried out the bulk of the acetylation experiments; E. S. and M. S. carried out the enzymatic biodegradability experiments; T. K. carried out the majority of the NMR measurements; A. T. carried out the strength-extensibility measurements; V. L. carried out the contact angle measurements; A. S. and K. S. prepared the nanopapers for acetylation and helped in data interpretation; A. S. carried out some acetylation experiments and helped in manuscript drafting; A. K. prepared the paper samples and helped in the interpretation of the results; H. O. and A. H. helped in the conception, drafting the manuscript and discussion of the results.

Conflicts of interest

There are no conflicts to declare.

Data availability

The data supporting this article have been included as part of the SI. Supplementary information: (1) detailed methods and experimental associated with determination of parameters (from NMR, SAXS-WAXS, AFM-IR & design of experiments), (2) a short molecular dynamics and diffraction pattern calculation regarding the mechanisms of acetylation. See DOI: **https://doi.org/10.1039/d5su00377f**.

References

1 C. J. Moore, M. K. Leecaster, S. L. Moore and S. B. Weisberg, A Comparison of plastic and plankton in the North Pacific Central Gyre, *Mar. Pollut. Bull.*, 2001, **42**, 1297.

2 J. Hammer, M. H. S. Kraak and J. R. Parsons, Plastics in the Marine Environment: The Dark Side of a Modern Gift, in *Reviews of Environmental Contamination and Toxicology*, ed. D. Whitacre, Springer, New York, NY, 2012, vol. 220.

3 A. Tajani and G. Ciamba, On the reduction of the impact of certain plastic products on the environment, *Off. J. Eur. Union*, 2019, **L155**, 1–19.

4 **https://eur-lex.europa.eu/eli/reg_del/2024/2770/oj**.

5 **https://eur-lex.europa.eu/eli/dec_impl/2019/665/oj/eng**.

6 J. E. Potts, R. A. Clendinning and W. B. Ackart, *An Investigation of the Biodegradability of Packaging Plastics*, EPA Study, 1972, EPA-R2-72-046.

7 N. Yadav and M. Hakkarainen M, Degradable or not? Cellulose acetate as a model for complicated interplay between structure, environment and degradation, *Chemosphere*, 2021, **265**, 128731.

8 J. Puls, S. A. Wilson and D. Hölter, Degradation of Cellulose Acetate-Based Materials: A Review, *J. Polym. Environ.*, 2011, **19**, 152.

9 E. L. Eronen-Rasimus, P. P. Näkki and H. P. Kaartokallio, Degradation Rates and Bacterial Community Compositions Vary among Commonly Used Bioplastic Materials in a Brackish Marine Environment, *Environ. Sci. Technol.*, 2022, **56**, 15760.

10 F. J. Ritter and J. Hartel, Qualitative, Quantitative and Preparative Chromatography of Steroids on Fully Acetylated Paper, *Nature*, 1958, **181**, 765.

11 T. A. Prevost, Thermally upgraded insulation in transformers, *Proceedings Electrical Insulation Conference and Electrical Manufacturing Expo*, Indianapolis, IN, USA, 2005, vol. 120.

12 L. Fliri, K. Heise, T. Koso, A. R. Todorov, D. Rico del Cerro, S. Hietala, J. Fiskari, I. Kilpeläinen, M. Hummel and A. W. T. King, Solution-state nuclear magnetic resonance spectroscopy of crystalline cellulosic materials using a direct dissolution ionic liquid electrolyte, *Prot. Nat.*, 2023, **18**, 2084.

13 M. Wojdyr, *Fityk*: A general-purpose peak fitting program, *J. Appl. Crystallogr.*, 2010, **43**(5), 1126.

14 T. Koso, M. Beaumont, B. Tardy, D. Rico del Cerro, S. Eyley, W. Thielemans, O. J. Rojas, I. Kilpeläinen and A. W. T. King, Highly regioselective surface acetylation of cellulose and shaped cellulose constructs in the gas-phase, *Green Chem.*, 2022, **24**, 5604.

15 M. Beaumont, P. Jusner, N. Gierlinger, A. W. T. King, A. Potthast, O. J. Rojas and T. Rosenau, Unique Reactivity of Nanoporous Cellulosic Materials Mediated by Surface-Confined Water, *Nat. Commun.*, 2021, **12**, 2513.

16 H. Steinmeier, 3. Acetate Manufacturing, Process and Technology: 3.1 Chemistry of Cellulose Acetylation, *Macromol. Symp.*, 2004, **208**, 49.

17 J.-F. Sassi and H. Chanzy, Ultrastructural aspects of the acetylation of cellulose, *Cellulose*, 1995, **2**, 111.

18 H. Kono, H. Hashimoto and Y. Shimizu, NMR characterization of cellulose acetate: Chemical shift assignments, substituent effects, and chemical shift additivity, *Carbohydr. Polym.*, 2015, **118**, 91.

19 T. Koso, M. Beaumont, B. Tardy, D. Rico del Cerro, S. Eyley, W. Thielemans, O. J. Rojas, I. Kilpeläinen and A. W. T. King, Highly regioselective surface acetylation of cellulose and shaped cellulose constructs in the gas-phase, *Green Chem.*, 2022, **24**, 5604.

20 A. D. French, Idealized powder diffraction patterns for cellulose polymorphs, *Cellulose*, 2014, **21**, 885.

21 P. Scherrer, Estimation of the Size and Internal Structure of Colloidal Particles by Means of Röntgen, *Nachr. Gesell. Wiss. Göttingen*, 1918, **2**, 96–100.

22 K. S. Salem, N. K Kasera, Md. A. Rahman, H. Jameel, Y. Habibi, S. J. Eichhorn, A. D. French, L. Pal and L. A. Lucia, Comparison and assessment of methods for cellulose crystallinity determination, *Chem. Soc. Rev.*, 2023, **52**, 6417.

23 P. Sikorski, M. Wada, L. Heux, H. Shintani and B. Stokke, Crystal Structure of Cellulose Triacetate I, *Macromolecules*, 2004, **37**, 4547.

24 K. Kobayashi, S. Kimura, E. Togawa and M. Wada, Crystal transition from cellulose II hydrate to cellulose II, *Carbohydr. Polym.*, 2011, **6**, 975.

25 A. Dazzi and C. B. Prater, AFM-IR: Technology and applications in nanoscale infrared spectroscopy and chemical imaging, *Chem. Rev.*, 2017, **117**, 5146.

26 C. Marcott, N. Lo, K. Kjolle, C. Prater and D. P. Gerrard, Applications of AFM-IR—Diverse Chemical Composition Analyses at Nanoscale Spatial Resolution, *Microsc. Today*, 2012, **20**, 16.

27 C. Marcott, M. Lo, K. Kjoller, F. Fiat, N. Baghdadli, G. Balooch and G. S. Luengo, Localization of Human Hair Structural Lipids Using Nanoscale Infrared Spectroscopy and Imaging, *Appl. Spectrosc.*, 2014, **68**, 564.

28 J. Wolfs, F. C. M. Scheelje, O. Matveyeva and M. A. R. Meier, Determination of the degree of substitution of cellulose esters via ATR-FTIR spectroscopy, *J. Polym. Sci.*, 2023, **61**, 2697.

29 A. Korpela, A. Tanakaand and A. W. T. King, A comparative study of the effects of chemical crosslinking agents on NBSK handsheet properties, *Bioresources*, 2023, **18**, 937.

30 I. Leppänen, M. Vikman, A. Harlin and H. Orelma, Enzymatic Degradation and Pilot-Scale Composting of Cellulose-Based Films with Different Chemical Structures, *J. Polym. Environ.*, 2020, **28**, 458.

31 T. Miyamoto, Y. Sato, T. Shibata, M. Tanahashi and M. Inagaki, 13c-Nmr Spectral Studies On The Distribution Of Substituents In Water-Soluble Cellulose Acetate, *J. Polym. Sci., Polym. Chem. Ed.*, 1985, **23**, 1373.

32 A. R. Todorov, A. W. T. King and I. Kilpeläinen, Transesterification of cellulose with unactivated esters in superbase-acid conjugate ionic liquids, *RSC Adv.*, 2023, **13**, 5983.

33 L. O. Klinga and E. L. Back, Wet strengthening of paper by partial acetylation. A new wet strengthening method, *Sven. Papperstidn.*, 1966, **69**, 64.

34 H. Kallakas, T. Kattamanchi, C. Kilumets, E. Tarasova, I. Krasnou, N. Savest, I. Ahmadian, J. Kers and A. Krumme, Tensile and Surface Wettability Properties of the Solvent Cast Cellulose Fatty Acid Ester Films, *Polymers*, 2023, **15**, 2677.

35 N. K. Kalita and M. Hakkarainen, Triggering Degradation of Cellulose Acetate by Embedded Enzymes: Accelerated Enzymatic Degradation and Biodegradation Under Simulated composting conditions, *Biomacromolecular*, 2003, **24**, 3290.